ISSN (Print) 1226-1750
ISSN (Online) 2233-6656
Journal of Magnetics 24(3), 402-407 (2019) https://doi.org/10.4283/JMAG.2019.24.3.402

Study of Dynamic Behaviors in a Spin Valve System Modeled by the Landau-Lifshitz-Slonczewski Equation

Javier A. Velez[1,2], Edward Mosso[3], and Omar J. Suarez[2]*

[1]*Corporación Universitaria del Caribe, Sincelejo, Colombia*
[2]*Universidad de Sucre, A. A. 406, Sincelejo, Colombia*
[3]*Departamento de Física, Facultad de Ciencias, Universidad de Tarapacá, Arica, Chile*

(Received 21 December 2018, Received in final form 31 August 2019, Accepted 17 September 2019)

In this work, the dynamic behavior of a spin valve oscillator with a Nickel-free layer, modeled by the Landau-Lifshitz-Slonczewski equation is studied. It is considered a constant applied field and a spin current with two components, a constant term and a term with a time-dependent harmonic modulation. Techniques to characterize dynamic behaviors of systems, such as Lyapunov exponents, bifurcation diagram, phase portraits, time series, and Fourier spectra were used. It is demonstrated that the system presents multiple transitions between chaotic and regular states when the constant magnetic field, the magnitude, and frequency of the alternating current are varied. Furthermore, it is found that the effect of the magnetic field and the amplitude of the currents play a meaningful role in the chaotic behavior start.

Keywords : Spin valve, Landau-Lifshitz-Slonczewski equation, chaotic states

1. Introduction

In recent years, numerous theoretical and experimental investigations on the dynamic properties of magnetization of magnetic nanoparticles have been encouraged by the potential technological applications that these particles might have. In spintronics, applications based on this principle combine electronics and magnetism by using the electron as a unit of charge plus the intrinsic spin of the electron as a magnetic unit [1-4]. A spin-polarized current flowing through a pinned magnetic layer can generate a Spin-Transfer Torque (STT) on a free ferromagnetic layer [5-7]. The STT is key to technological development that aims to fabricate the of magnetic random access memory (STT-MRAM) for ultrafast applications, employing ferromagnetic, ferrimagnetic, or antiferromagnetic materials [8-11]. The magnetic motions that exhibit the ferromagnetic free layer due to torque have been studied experimentally and theoretically. Magnetoresistance measurements made using samples of different magnetic material concentration (Co, Cu) forming a multi-layer structure have shown different dynamical regions on the phases diagram, magnetic field - current (H-I) such as stationary equilibrium region for the magnetization, and a steady magnetization precession region [12]. Micromagnetic simulations verify these observations, as well as the identification of a chaotic region [13]. The Landau-Lifshitz-Gilbert-Slonczewski (LLGS) equation models the temporal evolution of the magnetization on the free layer to zero temperature [14-16]. Different configurations of the spin-polarized current and the magnetic field have been considered in the spin-valve systems, observing different dynamical behaviors: a periodic dynamic with various periodicities, a quasi-periodic, and a chaotic. Numerical simulations have found that in these systems, the route to chaos is through a cascade of period-doubling bifurcations [17-19].

This work aims to provide a better understanding of the dynamic transitions occurring in an anisotropic magnetic free layer of a spin-valve system, due to a constant magnetic field and a time-dependent current density. Furthermore, this work clarifies the effects that the system control parameters have on the chaotic behavior inception. These results can motivate further experiments in this area.

The dynamical behavior of the system is analyzed using different dynamic indicators. The Lyapunov exponents, bifurcation diagrams, Fourier power spectra, phase portraits, and time series, which are potent techniques applied in previous works [20-26], are calculated. This article is

*Corresponding author: Tel: +57-5-2712929
Fax: +57-5-2712929, e-mail: omar.suarez@unisucre.edu.co

organized as follows: Section 2 presents the theoretical model description. Then, in Section 3, numerical results and analyses of them are shown. Finally, in Section 4, relevant conclusions of this investigation are stated.

2. Model

Let us consider a spin valve system consisting of three sandwich layers: two ferromagnetic layers separated by a non-ferromagnetic spacer layer. There is a constant external magnetic field $\mathbf{H}_E$ and an electrical current J_e with two components, a constant term and a term involving a time-dependent harmonic modulation. The electron's spin flowing into the spin valve does not have a preferred polarization, i.e., the spin current is not polarized. However, the spin distributions acquire a partial polarization for those electrons that flow into the first ferromagnetic layer with pinned magnetization in the $\hat{\boldsymbol{p}}$ direction. These electrons continue their way through the spacer layer and eventually arrive at the second free ferromagnetic layer (that will be considered as a magnetic monodomain). Upon their arrival, the spin-polarized current interacts with the monodomain, exerting a torque on the magnetization, transferring an angular momentum (Spin-Transfer Torque), finally influencing the monodomain orientation. The dimensionless Landau-Lifshitz (LL) equation [27, 28] is used to study the magnetization dynamics of this free layer, and the spin-transfer torque associated with the polarized current of spin in the manner proposed by Slonczewski [5, 6] is considered. This equation is given by

$$\frac{d\mathbf{m}}{d\tau} = -\mathbf{m}\times\mathbf{h}_{\text{eff}} - \alpha\,\mathbf{m}\times(\mathbf{m}\times\mathbf{h}_{\text{eff}}) + \tilde{\beta}\,\mathbf{m}\times(\mathbf{m}\times\hat{\mathbf{p}}), \quad (1)$$

where the magnetization and effective field are in units of the saturation magnetization M_s, ($\mathbf{m} = \mathbf{M}/M_s$ and $\mathbf{h}_{\text{eff}} = \mathbf{H}_{\text{eff}}/M_s$), and time in units of $(|\gamma|M_s)^{-1}$, that is, the dimensionless time $\tau = |\gamma|M_s t$ is defined. Here the saturation magnetization leads to $|\mathbf{m}| = 1$. The factor α is the damping coefficient, and $|\gamma|$ is the gyromagnetic factor associated with the electron spin and its numerical value is approximately given by $|\gamma| \approx 2.21 \times 10^5$ m/As. The last term in equation (1) corresponds to the spin-torque with $\tilde{\beta} = g(\mathbf{m}\cdot\hat{\mathbf{p}})J_e/J_P$, where J_e represents the applied current density taken as positive when the electrons flow from the free to the fixed layer [14], J_p is a parameter with dimensions of current density given by $J_P = \mu_0 M_s^2 |e| l/\hbar$ where $|e|$ is the absolute value of the charge of the electron, l is the thickness of the free layer, which has been taken with a value of 3 nm and, $\hbar$ is the reduced Planck constant. The spin-transfer efficiency is a function of the dot product $\mathbf{m}\cdot\hat{\mathbf{p}}$ and it is given by $g(\mathbf{m}\cdot\hat{\mathbf{p}}) = [f(P)(3+(\mathbf{m}\cdot\hat{\mathbf{p}})) - 4]^{-1}$ with $f(P) = (1+P)^3/4P^{3/2}$, where P represents the degree of polarization of the electrons coming from the fixed layer [14], in our case $\hat{\mathbf{p}} \| \hat{\mathbf{z}}$.

Table 1. Simulation parameters for the Ni-based alloys.

M_s (A/m)	P	K_0 (J/m^3)	$\|\gamma\|M_s$ (ps)	J_P (A/m^2)
4.80×10^5	0.11	5.3×10^3	9.4	1.32×10^{12}

In this scenario, an external magnetic field and a free layer with uniaxial anisotropy are considered. The effective magnetic field $\mathbf{h}_{\text{eff}}$ is written as $\mathbf{h}_{\text{eff}} = \mathbf{h}_E - \beta(m_x\hat{\mathbf{x}} + m_y\hat{\mathbf{y}})$, where $\mathbf{h}_E = \mathbf{H}_E/M_s = h_0\hat{\mathbf{x}}$ is the external field and $\beta = \mathbf{H}_K/M_s$ is the measure of the anisotropy, where $\mathbf{H}_K = 2K_0/M_s$ with K_0 is the anisotropy constant. In this case, the easy axis is parallel to the z-direction. Furthermore, it is assumed the normalized current as $J_e/J_P = I_0 + I_1\sin(\Omega_c\tau)$, where I_0, I_1, and Ω_c are dimensionless constants expressed as $I_0 = J_e^0/J_P$, $I_1 = J_e^1/J_P$, and $\Omega_c = w_c/|\gamma|M_s$; being J_e^0, and J_e^1 the amplitudes of the constant and time-dependent current densities, respectively and Ω_c the normalized frequency. The dynamical behaviors of a spin valve oscillator, considering the free layer of Nickel material are characterized. Typical experimental values for this material with their corresponding time scale are shown in Table 1.

3. Simulations

This section is divided into two parts. The first subsection introduces the characterization techniques employed to analyze the dynamical behavior of the system. The second subsection presents the results and their discussion.

3.1. Techniques of dynamical characterization

The dynamic system described by Eq. (1) under the action of a time-dependent current of the form defined in this work cannot be solved analytically. This issue is due to non-linear and temporal dependencies. The system of differential equations associated with Eq. (1) is solved numerically using the fourth-order Runge-Kutta method with a time step $d\tau = 0.1$ and precision of 10^{-8} for the magnetic moment. The dynamic system employing the Lyapunov exponents (LEs) is characterized. This technique consists of quantifying the divergence between two trajectories with initial conditions that are very close to each other. Accordingly, i-th Lyapunov exponent λ_i, of a dynamic system of effective dimension N described by a set of equations of the form, $dX^i/dt = F^i(X, t)$, is given by:

$$\lambda_i = \lim_{\tau\to\infty}\frac{1}{\tau}\left(\frac{\|\delta X_\tau^i\|}{\|\delta X_0^i\|}\right), \quad (2)$$

where δX^i_ξ is the distance between the trajectories of the i-th component of the vector field in time. The time $\tau \to \infty$ in the previous expression must be interpreted as the necessary ξ time, sufficiently large, such that the separation of the trajectories reaches its saturation value, which will be limited by the diameter of the attractor. These exponents can be ordered, from the largest to the smallest: $\lambda_1 \geq \lambda_2 \geq \ldots \geq \lambda_N$. The first exponent, λ_1, is known as the largest Lyapunov exponent (LLE). By exploring the dependence of the LLE with the different parameters of the system, regions can be identified in the parameter space where the dynamics are chaotic (positive LLE), or where non-chaotic dynamics are present (zero or negative LLE) [21, 29]. A classification of the dynamic behaviors of a time-continuous system regarding the spectrum of Lyapunov indicates that to observe a chaotic behavior it is necessary that the system has, at least, dimension-3. While in systems of dimension-1, there are fixed points; in systems of dimension-2, one can find periodic attractors type limit cycle, in addition to fixed points. The system has dimension-3, so it is possible to find interesting dynamic behaviors such as quasi-periodic or chaotic behaviors. The calculation of the Lyapunov exponents is one of the most used techniques as an indicator of chaos. In this work, these exponents are relevant to our analysis because they allow visualizing and delimit the different dynamic regions where the system presents chaotic and regular behavior when the different parameters of the system are varied.

In addition to this method, other indicators of quantifying the dynamical behaviors of a system, such as the computation of bifurcation diagrams, Fourier spectrum, phase portraits, and time series, are used. Bifurcation diagrams have been previously used to quantify the nonperiodic behavior of a dynamical system [24, 25]. A bifurcation diagram enables one to elucidate the transition dynamics that exhibit the system when a control parameter is varied. The bifurcation diagram is obtained by repeatedly taking the maximum value of the time series of the m_y component, calculated for a time span of $\tau = 5000$ after removing the transient portion of the motion.

3.2. Results

To elucidate the dynamical transitions that exhibit a spin valve oscillator, the focus is on three parameters: the time-dependent current amplitude I_1, the normalized frequency Ω_c, and the constant magnetic field h_0. The constant current amplitude at $I_0 = 0.10$ and the dissipation parameter at $\alpha = 0.02$ are fixed. The regions in the parameter space where chaotic and regular behaviors are found are delimited. Numerical simulations are performed with the parameters presented in Table 1.

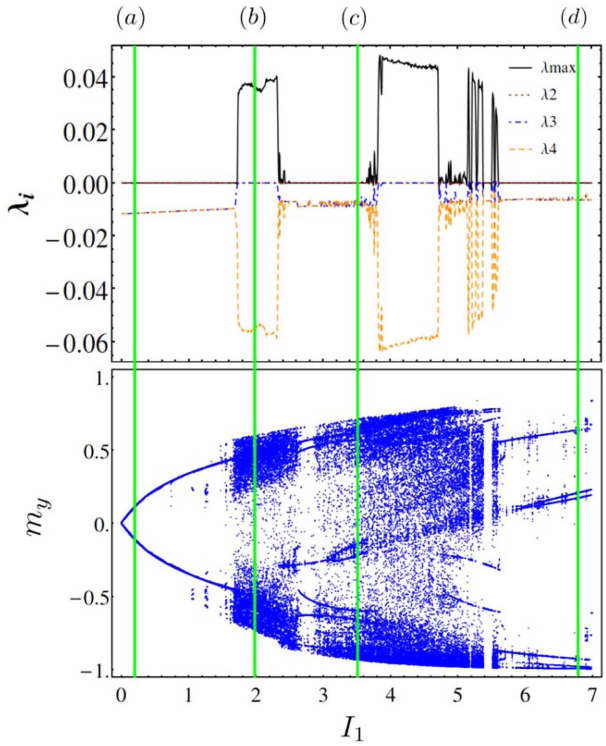

Fig. 1. (Color online) Lyapunov spectrum and bifurcation diagram of the magnetization vector as a function of the current amplitude I_1. Fixed parameters: $h_0 = 0.06$ and $\Omega_c = 0.30$. The physical values of the parameters are $H_E = 0.036$ T, $\omega_c = 31.8$ GHz, and $J_e^0 = 1.32 \times 10^{11}$ A/m^2.

Figure 1 shows the Lyapunov exponents and the bifurcation diagram as a function of I_1. In this figure, the LLE, λ_{max}, corresponds to the solid line, the other three exponents λ_2, λ_3 and λ_4, corresponding to dotted, dot-dashed and dashed lines, respectively. The fixed values of the constant magnetic field and normalized frequency are $h_0 = 0.06$ and $\Omega_c = 0.30$, respectively. It is observed that when the current I_1 takes values between $0 < I_1 < 1.7$, the LLE is positive, and the system exhibits periodic states. When the current is in the range, $1.7 < I_1 < 5.6$, the system presents multiple transitions between chaotic and regular states. In this zone, it can be observed that the boundaries that separate regions from chaotic and regular states can be very complicated. For values higher than $I_1 = 5.6$ and less than 7.0, the LLE becomes zero, the magnetization of the free layer presents a purely regular behavior. Additionally, with the comparison of the LLE and the bifurcation diagram, one can determine precisely the segments where the regular phases correspond to periodic or quasi-periodic behaviors. For instance, in ranges $0 < I_1 < 1.7$ and $I_1 > 5.6$, the dynamical behaviors are periodic as indicate the LLE. In the range, $2.43 < I_1 <$

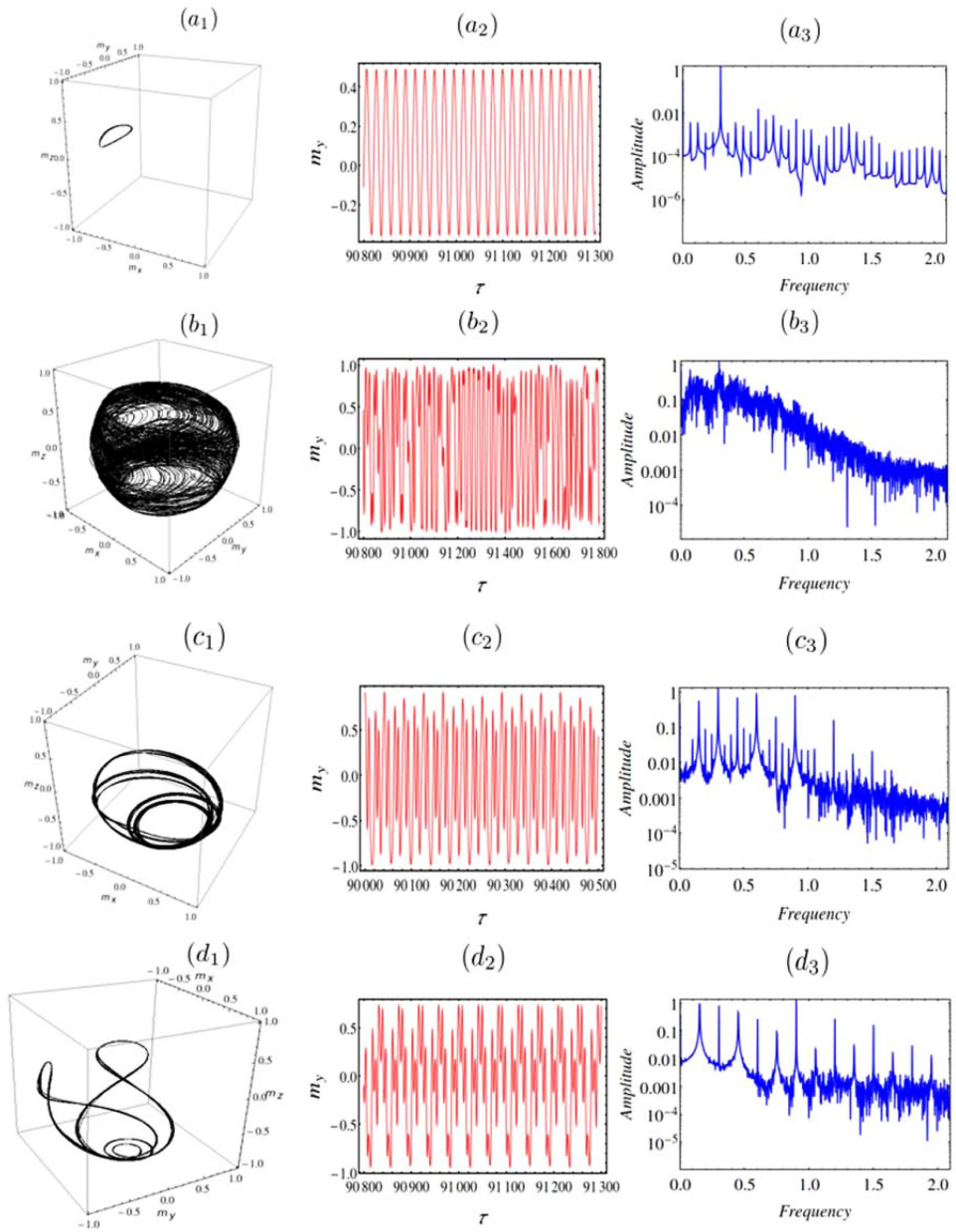

Fig. 2. (Color online) (1) Phase portrait, (2) time series for m_y and (3) Fourier spectrum for four values of, I_1, (a) I_1 = 0.20, (b) I_1 = 2.00, (c) I_1 = 3.50 and (d) I_1 = 6.80 respectively. Fixed parameters are the same as those in Fig. 1. The physical values of the parameters are (a) $J_e^1 = 2.64 \times 10^{11}$ A/m^2, (b) $J_e^1 = 2.64 \times 10^{12}$ A/m^2, (c) $J_e^1 = 4.55 \times 10^{12}$ A/m^2, and (d) $J_e^1 = 8.98 \times 10^{12}$ A/m^2.

3.64, the LLE is null, quasi-periodic oscillations can be identified, except for a region, (2.65, 2.94), where the dynamic is periodic. It is remarked that different dynamical behaviors in spin-valve systems have been reported such as chaotic dynamics, periodic and quasiperiodic dynamics [17-19, 26, 30]. It is essential to have a sound understanding of the effect of the time-dependent currents on the dynamic states since higher currents can lead to undesirable consequences such as excessive heating in the system, and therefore modify the dynamic states.

Figure 2 shows the phase portrait, the time series of m_y, and its corresponding Fourier spectrum, for four particular cases of current amplitude I_1, which are marked in Fig. 1 with a green line, namely 0.20, 2.00, 3.50, and 6.80.

Figure (a), shows a purely periodic state for small values of the current, I_1 = 0.20, with LLE null. The Fourier spectrum is made in logarithmic scale, whereby it is observed one principal characteristic frequency. Figure (b) shows the results obtained for a value of current of I_1 = 2.00 with a positive LLE. The system is found in a

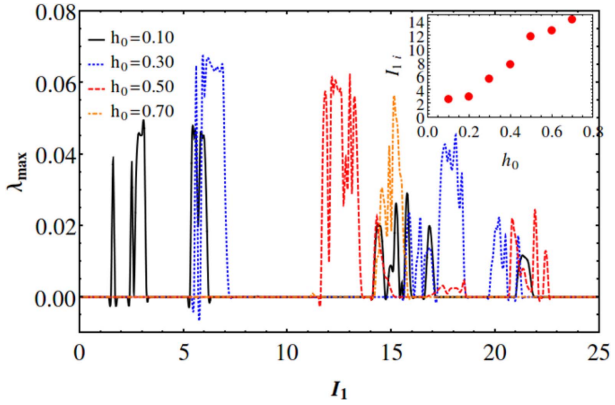

Fig. 3. (Color online) Lyapunov spectrum as a function of the current amplitude I_1 for four values of the magnetic field $h_0 = 0.10$, $h_0 = 0.30$, $h_0 = 0.50$ and $h_0 = 0.70$. Fixed parameters are the same as those in Fig. 1. The physical values of the parameters are, $H_E = 0.180$T, $H_E = 0.301$ T, $H_E = 0.036$ T, and $H_E = 0.422$ T.

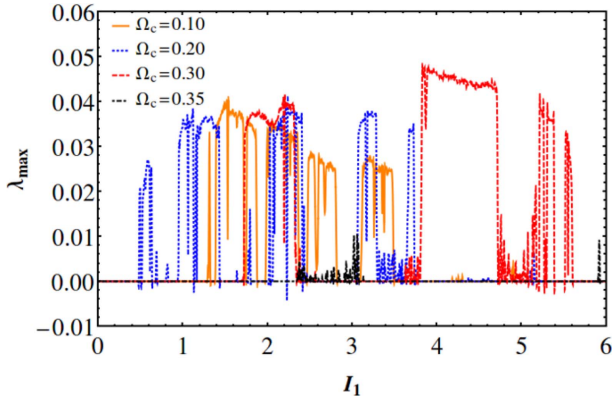

Fig. 4. (Color online) Lyapunov spectrum for four frequency values $\Omega_c = 0.10$, $\Omega_c = 0.20$, $\Omega_c = 0.30$ and $\Omega_c = 0.35$, as a function of the I_1 current amplitude. Fixed parameters are the same as those in Fig. 1. The physical values of the parameters are $\omega_c = 10.6$ GHz, $\omega_c = 21.2$ GHz, $\omega_c = 31.8$ GHz, and $\omega_c = 37.1$ GHz.

chaotic state. In Fig. (b_1) it can be seen how the movement of the magnetization vector **m**, associated with the free layer, fills a large zone of the phase space. Figure (b_2), shows the temporal evolution of the m_y component describing an aperiodic movement, and the Fourier spectrum shows a continuum set of characteristic frequencies, which corroborate the behavior observed in the phase diagram. Figures (c) and (d) show results for the bifurcation diagram region where the LLE is null; the values of currents are $I_1 = 3.50$ and $I_1 = 6.80$, respectively. In these cases, the system exhibits nonchaotic states, which are regular but different from each other. Figure (c) corresponds to a regular state; but in this case, the behavior is a quasiperiodic state. In fact, from the Fourier spectra, the presence of multiple modes can be observed. In Fig. (d), the magnetization **m** describes a multi-periodic behavior since the Fourier spectra show a discrete rational number of frequencies.

Figure 3 shows the LLE as a function of the current I_1 for different values of the magnetic field h_0, represented by solid, dotted, dashed, and dot-dashed lines. The frequency value is fixed as was done in Fig. 1. The effects of the constant magnetic field on the chaotic behavior start are analyzed. Results show that for all the magnetic field values to lower values of the current I_1, the dynamical behavior system is always a regular state. Furthermore, the chaotic state starts first at lower values of the I_1 for lower values of the magnetic field, $h_0 = 0.10$. When the field is increased, the chaotic behavior appears at higher current. The inset shows the values of the constant magnetic field and a time-dependent current amplitude when the chaotic behavior starts. For higher magnetic field, the current necessary for chaos to appear will be higher. The frequency effect on the dynamical behavior of the system is shown in the following figure.

Figure 4 shows the LLE as a function of the current I_1 for different frequency values Ω_c represented by solid, dotted, dashed, and dot-dashed lines. The constant magnetic field value is fixed as was done in Fig. 1. In contrast to the previous case; the chaotic state start, as a function of the time-dependent current amplitude, follows a non-uniform behavior when the frequency values are increased. From the Lyapunov exponents, one can observe that there are multiple transitions among chaotic and regular states. In all cases, to high and low currents and frequencies values, the dynamical behaviors of the system are purely regular. Moreover, the system exhibits different types of regular states, being the cyclic states with different periodicities.

4. Conclusions

In this article, the dynamic behavior of a spin valve oscillator in the presence of a constant magnetic field and a current with two components, a constant component, and a time-dependent component is described numerically. The temporal evolution of the magnetization is modeled by the Landau-Lifshitz-Slonczewski equation, which describes with accuracy the dynamic behavior of a spin valve oscillator. Efforts have been concentrated on understanding the impact of the constant magnetic field, the current amplitude, and the frequency on the dynamical behaviors of the system. The Lyapunov exponents, bifurcation diagrams, phase portraits, time series, and Fourier

power spectra were applied to characterize dynamics of the system. Simulations results show that the magnetization of the free layer follows a dynamic behavior which presents multiple transitions between chaotic and regular states. Periodic behavior of the system was registered when the time-dependent current amplitude is low, and hence as it increases, the system exhibits transitions to chaotic states; while for high values of current, the system returns to regular states.

Furthermore, results demonstrate that the chaos onset strongly depends on the control parameters leading us to conclude that for higher values of the constant magnetic field, the higher the amplitudes of the time-dependent currents will be, which are required for the chaos inception. However, this same effect is not observed when frequency increases; at a higher frequency the current amplitudes that are required do not follow a monotonous pattern. Finally, it is highlighted that the chosen parameters are within the experimental range therefore, it is believed that these states could be detected experimentally.

Acknowledgments

E. Mosso was supported by Comisión Nacional de Investigación Científica y Tecnológica (CONICYT, FONDECYT Grant No. 11160894, Chile) Convenio de Desempeño FIP UTA1309 and Convenenio Marco FID UTA1756.

References

[1] J. A. Katine and E. E. Fullerton, J. Magn. Magn. Mater. **320**, 1217 (2008).
[2] P. Grünberg, R. Schreiber, Y. Pang, M. B. Brodsky, and H. Sowers, Phys. Rev. Lett. **57**, 2442 (1986).
[3] M. N. Baibich, J. M. Broto, A. Fert, F. Nguyen Van Dau, F. Petroff, P. Etienne, G. Creuzet, A. Friederich, and J. Chazelas, Phys. Rev. Lett. **61**, 2472 (1988).
[4] S. D. Bader and S. S. P. Parking, Annu. Rev. Condens. Matter Phys. **1**, 71 (2010).
[5] J. C. Slonczewski, J. Magn. Magn. Mater. **159**, L1 (1996).
[6] L. Berger, Phys. Rev. B **54**, 9353 (1996).
[7] D. C. Ralph and M. D. Stiles, J. Magn. Magn. Mater. **320**, 1190 (2008).
[8] S. Parkin and S. H. Yang, Nature Nanotech. **10**, 195 (2015).
[9] A. J. Schellekems, K. C. Kuiper, R. R. J. C. De Wit, and B. Koopmans, Nat. Commun **5**, 4333 (2014).
[10] K. Y. Camsari, A. Z. Pervaiz, R. Faria, E. E. Marinero, and S. Datta, IEEE Magn. Lett. **7**, 3107205 (2016).
[11] V. Baltz, A. Manchon, M. Tsoi, T. Moriyama, T. Ono, and Y. Tserkovnyak, Rev. Mod. Phys. **90**, 015005 (2018).
[12] S. I. Kiselev, J. C. Sankey, I. N. Krivorotov, N. C. Emley, R. J. Schoelkopf, R. A. Buhrman, and D. C. Ralph, Nature **425**, 380 (2003).
[13] K. J. Lee, A. Deac, O. Redon, J. P. Nozières, and B. Dieny, Nature Mater. **3**, 877 (2004).
[14] I. D. Mayergoyz, G. Bertotti, and C. Serpico, Nonlinear Magnetization Dynamics in Nanosystems, Elsevier, Dordrecht, (2009).
[15] D. V. Berkov, J. Miltat. J. Magn. Magn. Mater. **320**, 1238 (2008).
[16] P. Gambardella and J. M. Miron. Phil. Trans. R. Soc. A **369**, 3175 (2011).
[17] Z. Yang, S. Zhang, and Y. C. Li, Phys. Rev. Lett. **99**, 134101 (2007).
[18] S. Murugesh and M. Lakshmanan, Chaos **19**, 043111 (2009).
[19] P. P. Horley, M. Y. Kushnir, M. Morales-Meza, A. Sukhov, and V. Rusyn, Physica B **486**, 60 (2016).
[20] L. F. Alvarez, O. Pla, and O. Chubykalo, Phys. Rev. B **61**, 11613 (2000).
[21] J. Bragard, H. Pleiner, O. J. Suarez, P. Vargas, J. A. C. Gallas, and D. Laroze, Phys. Rev. E **84**, 037202 (2011).
[22] D. Laroze, D. Becerra-Alonso, J. A. C. Gallas, and H. Pleiner, IEEE Trans. Magn. **48**, 3567 (2012).
[23] L. M. Pérez, J. Bragard, H. L. Mancini, J. A. C. Gallas, A. M. Cabanas, O. J. Suarez, and D. Laroze, Netw. Heterog. Media **10**, 209 (2015).
[24] A. M. Ferona and R. E. Camley, Phys. Rev. B **95**, 104421 (2017).
[25] O. J. Suarez, D. Laroze, J. Martínez-Mardones, D. Altbir, and O. Chubykalo-Fesenko, Phys. Rev. B **95**, 014404 (2017).
[26] A. M. Cabanas, L. M. Pérez, and D. Laroze, J. Magn. Magn. Mater. **460**, 320 (2018).
[27] L. D. Landau, E. M Lifshitz. Physik Zeiten der Sowietunion **8**, 153 (1935).
[28] T. L. Gilbert, Physical Review **100**, 1243 (1955).
[29] S. H. Strogatz, Nonlinear dynamics and chaos, second edition, Westview Press (2015).
[30] J. Cai, Y. Kato, A. Ogawa, Y. Harada, M. Chiba, and T. Hirata, J. Phys. Soc. Jap. **71**, 3087 (2002).